Molecular Crystals and Liquid Crystals

ISSN: 1542-1406 (Print) 1563-5287 (Online) Journal homepage: http://www.tandfonline.com/loi/gmcl20

Improvement of luminous efficiency using LI-doped MgO layer coated by MgCaO crystal powders in plasma display panels

Choon-Sang Park, Eun Young Jung & Heung-Sik Tae

To cite this article: Choon-Sang Park, Eun Young Jung & Heung-Sik Tae (2017) Improvement of luminous efficiency using LI-doped MgO layer coated by MgCaO crystal powders in plasma display panels, Molecular Crystals and Liquid Crystals, 645:1, 130-137, DOI: 10.1080/15421406.2016.1277496

To link to this article: https://doi.org/10.1080/15421406.2016.1277496

MOLECULAR CRYSTALS AND LIQUID CRYSTALS
2017, VOL. 645, 130–137
http://dx.doi.org/10.1080/15421406.2016.1277496

Taylor & Francis
Taylor & Francis Group

Improvement of luminous efficiency using LI-doped MgO layer coated by MgCaO crystal powders in plasma display panels

Choon-Sang Park[a], Eun Young Jung[b], and Heung-Sik Tae[a]

[a]School of Electronics Engineering, College of IT Engineering, Kyungpook National University, Daegu, South Korea; [b]Core Technology Lab, Corporate R&D Center, Samsung SDI Company Ltd., Cheonan, Chungcheongnam-Do, South Korea

ABSTRACT

In this study, the influences of the Li-doped MgO layer sprayed by MgCaO crystal powders on the discharge and luminous efficiency characteristics are examined under the high Xe (= 30%) gas condition in 6-in. test alternating-current plasma display panels (ac-PDPs) with 50-in. full-high definition (FHD) cell size. Our experimental results reveal that spraying the MgCaO crystal powders on the Li-500 ppm doped MgO layer can reduce the firing voltage considerably by about 60 V under the high Xe (= 30%) gas condition. As a result, the maximum luminous efficacy of about 40% improvement is obtained when adopting the Li-500 ppm doped MgO layer coated by MgCaO crystal powders under high Xe (= 30%) gas condition.

KEYWORDS

Plasma display panel; high xe; MgCaO crystal powder; LI-doped MgO layer; functional layer; luminance; firing voltage; discharge current; luminous efficiency

1. Introduction

The MgO layers have been used as a protective layer in ac plasma display panels (ac-PDPs) due to their high stability against ion bombardment, low optical loss, high thermal stability, and good electrical insulating properties. Moreover, the MgO layers play a significant role in reducing the discharge voltage of ac-PDPs due to their high secondary electron emission capability and thus, various attempts to improve the characteristics of these layers have been reported [1–11]. Nevertheless, it is still necessary to improve the luminous efficacy to survive in the flat panel display market. For improving luminous efficiency of ac-PDPs, in cases of increasing the Xe gas partial pressure, the corresponding discharge characteristics, especially firing voltage, are much aggravated under the conventional MgO layer [12–15]. Therefore, the research of various types of MgO crystal powder on the conventional MgO layer, which is called a functional layer, is needed to overcome the demerits of the conventional MgO layer.

Accordingly, in this study, the newly proposed MgCaO crystal powders sprayed on the conventional MgO layer are examined to overcome the demerits of the conventional MgO layer especially under the high Xe (= 30%) gas condition in the 6-in. test PDP panel with 50-in. full-high definition (FHD) cell size. Additionally, Li-doped MgO layer is employed to more improve the MgO characteristics especially under the high Xe (= 30%) gas condition. The corresponding discharge and luminous efficiency characteristics are analyzed and

CONTACT Heung-Sik Tae hstae@ee.knu.ac.kr
Color versions of one or more of the figures in the article can be found online at www.tandfonline.com/gmcl.

Table 1. Specifications of 6-in. test panel with 50-in. FHD cell size employed in this study.

Front panel		Rear panel	
ITO width	120 μm	Barrier rib width	50 μm
ITO gap	50 μm	Barrier rib height	120 μm
Bus width	40 μm	Address width	85 μm
Cell pitch		192 μm $\times$ 576 μm	
Barrier rib type		Closed rib, single rib	
Gas Pressure		420 Torr	
Gas chemistry		Ne-Xe (30%)-He (30%)	

compared relative to the Li-doping rates for both the MgO layers with and wihout MgCaO crystal powders.

2. Experiment set-up

The 6-in. test panel has three electrodes where X is the sustain electrode, Y is the scan electrode, and A is the address electrode [14–16]. The gas pressure and gas mixture of the test panel are 420 Torr and Ne-He (30%)-Xe (30%), respectively. The detailed specifications of the 6-in. test panel with 50-in. FHD cell size employed in this study are given in Table 1. The luminance and discharge current are measured by using a color analyzer (Konika Minolta, CA-100 plus) and power meter (WT210), respectively. The IR emissions for V_t closed curve [9,10,17,18] are measured by using the photosensor amplifier (Hamamatsu C6386) and VTC 2.0 (Future Technology Lab., Wall Charge Measurement System). The sustain frequency and the duty ratio of the sustain pulses for the sustain period are 200 kHz and 40%, respectively. The MgO thin films are prepared by the MgO pellet (high purity 99.99%) as evaporation source and deposited by the e-beam evaporation method under oxygen(O_2) flow rate of about 15 standard cubic centimeters per minute (sccm) with respect to Li doping rates. The Li doping rate in the MgO layer is changed from 200 to 1000 parts per million (ppm). The MgCaO crystal powder is coated on the Li-doped MgO surface by a spray method in ac-PDPs. The X-ray diffraction (XRD) and field emission scanning electron microscopy (FE-SEM) are used to estimate the dependence of the film crystallinity and analyze the surface morphology, respectively.

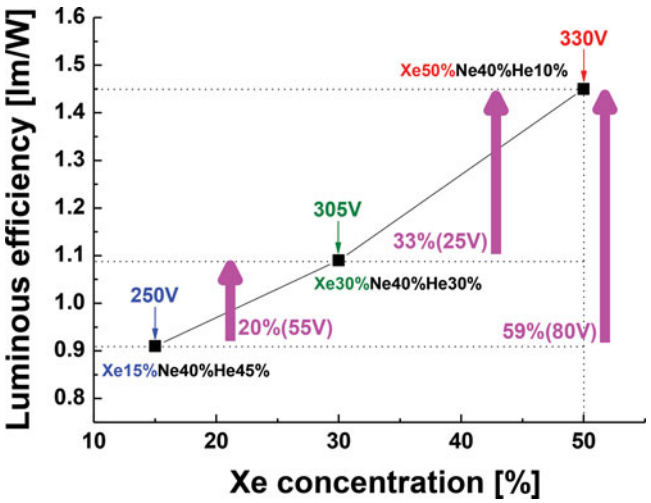

Figure 1. Changes in luminous efficiency and sustain discharge voltage as variations of Xe concentration from 15 to 50% in 6-in. test panel with 50 in FHD cell size and conventional MgO layer.

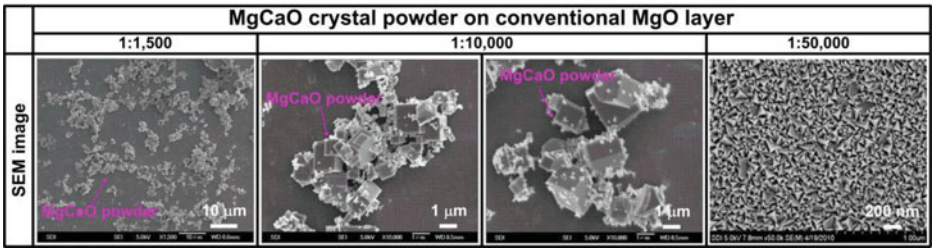

Figure 2. SEM images of MgCaO crystal powders on conventional (Ref.) MgO layer.

3. Results and discussion

Figure 1 shows the changes in the luminous efficiency and sustain discharge voltage as variations of Xe concentration from 15 to 50% in the 6-in. test panel with 50-in. FHD cell size and conventional MgO layer. As shown in Fig. 1, the luminous efficiency became more enhanced in proportion to an increase in the Xe%. An increase in the Xe% means a decrease in the He% because the Ne content in this study was fixed at 40%. In view of luminous efficacies, the increase in the Xe% is necessary, however, the sustain voltage is also remarkably increased in the case of using the conventional MgO layer, thereby resulting in producing unstable discharge [not shown here]. Accordingly, in this study, the additional MgCaO crystal powder is sprayed on the conventional MgO layer in order to overcome the demerits of the conventional MgO layer such as the considerable increase in the higher Xe (>20%) gas partial pressure.

Figure 2 shows the SEM images at low and high magnifications of MgCaO crystal powder sprayed on the conventional MgO layer. As shown in Fig. 2, in this experiment, the MgCaO crystal powders have sizes ranging from a few tens of nanometers to a few micrometers, and the MgCaO crystal powders have an about 8 wt% deposited area over the entire MgO surface. A few micrometers sizes of the MgCaO crystal powder are shown in the cubic shape of Fig. 2.

Figure 3 shows the XRD patterns of the MgO layer without and with MgCaO crystal powders. As shown in the XRD pattern of Fig. 3, the (200) peak is newly detected, which is mainly due to the presence of MgCaO crystal powders, whereas another peaks do not show any marked changes in the positions of the (111) and (222) peaks.

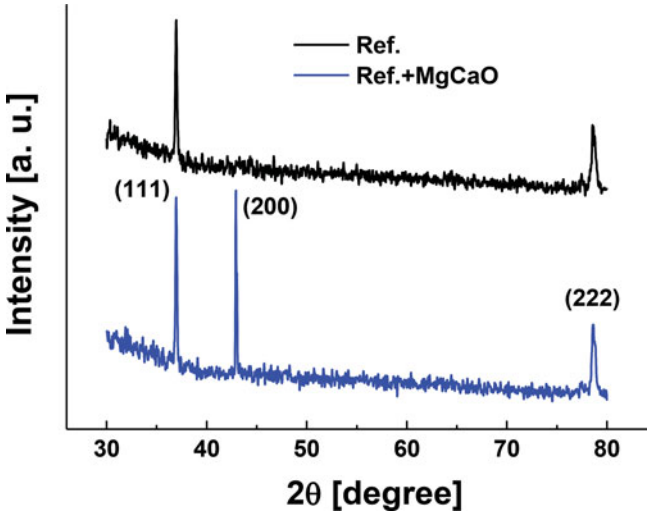

Figure 3. XRD patterns of MgO layer without and with MgCaO crystal powders.

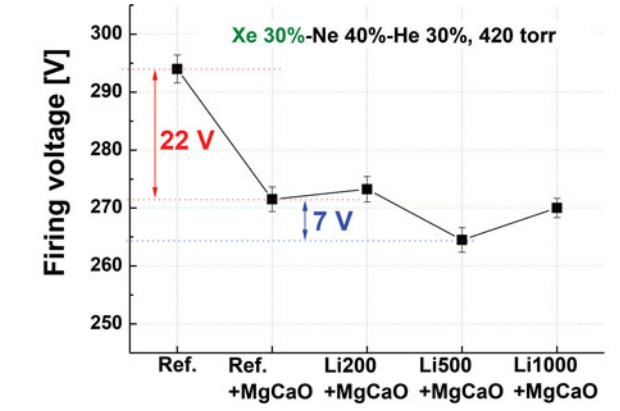

(a)

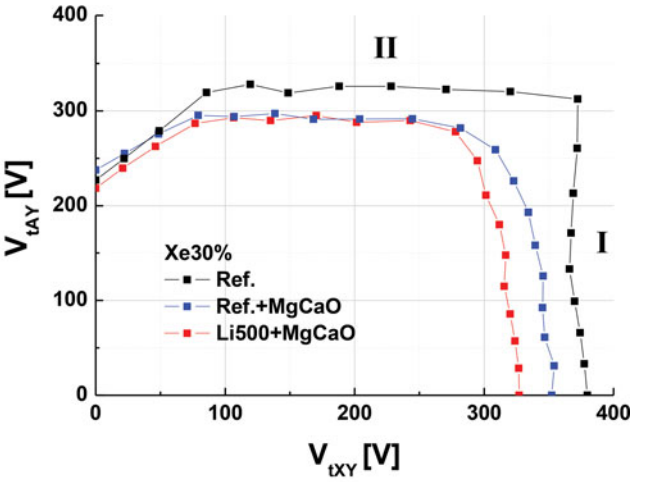

(b)

Figure 4. (a) Changes in firing voltages under high Xe (= 30%) without and with MgCaO crystal powders on MgO layer doped by various Li doping rates, and (b) V_t closed curves measured from 6-in. test panel with high Xe (= 30%) gas condition without and with MgCaO crystal powders on MgO layer doped by various Li doping rates, where I: V_{tXY} (= discharge start threshold cell between X and Y) and II: V_{tAY} (= discharge start threshold cell between A and Y), both sides I and II are threshold voltages under MgO cathode discharge conditions.

Figure 4 (a) shows the firing voltages during a sustain period including the reset and address periods with high Xe (= 30%) without and with MgCaO crystal powders on the MgO layers doped by various Li doping rates. Figure 4 (b) shows the changes in the V_t closed curves under no initial wall charge condition in the 6-in. test panels with high Xe (= 30%) without and with MgCaO crystal powders and Li-500 ppm doped MgO layer with MgCaO powders. The firing voltages for sides I (X-Y) and II (A-Y) are measured under the MgO cathode conditions from the 6-in. test panels. The corresponding values obtained from the V_t closed curves of Fig. 4 (b) are listed in Table 2. As shown in Fig. 4, the Li-doped MgO layer is additionally used instead of the conventional MgO, that is, the MgO that do not dope the Li, in order to further improve the MgO characteristics in the case of spraying the MgCaO crystal powders.

Table 2. Firing voltages measured from test panels based on V_t closed curves in Fig. 4 (b).

Region (MgO cathode)	Firing voltage (V)		
	Without (Ref.)	With MgCaO crystal powders	Li-500 ppm doped MgO layers with MgCaO
I	369	334	312
II	319	297	290

The discharge voltage is reduced by about 22 V in the case of spraying the MgCaO crystal powders when compared with that in the conventional MgO layer without MgCaO crystal powders in Fig. 4 (a). Furthermore, in the case of spraying the MgCaO crystal powders on the Li-doped MgO layer with proper ppm, that is, 500 ppm, the discharge voltage is observed to be more reduced by about 7 V. As shown in Fig. 4 (b) and Table 2, when spraying the MgCaO crystal powders, the firing voltages under MgO cathode conditions are lowered significantly. In cases of spraying the MgCaO crystal powders on the Li-500 ppm doped MgO layer, the firing voltage for side I is remarkably reduced by about 60 V, when compared with that of the conventional MgO layer. Thus, this experimental result confirms that spraying the MgCaO crystal powders on the Li-doped MgO layer can reduce the firing and discharge voltages especially under the high Xe (= 30%) gas condition.

Figure 5 shows the changes in the luminance, discharge current, and luminous efficiency measured from the 6-in. test panel with high Xe(= 30%) gas condition under various MgO surface conditions, that is, undoped MgO surface without MgCaO crystal powders (Ref.), undoped MgO surface with MgCaO crystal powders (Ref. + MgCaO), Li-doped (200 ppm) MgO surface with MgCaO crystal powders (Li200 + MgCaO), Li-doped (500 ppm) MgO surface with MgCaO crystal powders (Li500+MgCaO), and Li-doped (1000 ppm) MgO surface with MgCaO crystal powders (Li1000 + MgCaO). As shown in Fig. 5 (a), when comparing two cases, Ref. and Ref.+MgCaO cases, the luminance is significantly increased in the Ref. + MgCaO case. Furthermore, when spraying the MgCaO crystal powders on the Li-500 ppm doped MgO layer, the corresponding luminance is more increased, as also shown in Fig. 5 (a). Whereas, when spraying the MgCaO crystal powders on the Li-1000 ppm doped MgO layer, the luminance is decreased, when compared with that of the Li-500 ppm case, presumably due to the increase in the firing voltage shown in Fig. 4 (a) caused by degradation of the unique MgO layer with excessive Li doping. For the discharge current, when spraying the MgCaO crystal powders on the conventional MgO layer, the discharge current is slightly increased, as shown in Fig. 5 (b). However, when spraying the MgCaO crystal powders on the Li-1000 ppm doped MgO layer, the discharge current is considerably increased. As a result, the maximum luminous efficacy of about 40% improvement is obtained when adopting the Li-500 ppm doped MgO layer coated by MgCaO crystal powders under high Xe (= 30%) gas condition, as shown in Fig. 5 (c).

Based on the experimental results, the schematic model for the energy band diagrams in Fig. 6 is proposed for the conventional (i.e., undoped MgO layer) and Li-doped MgO layer. It is well known that the firing voltage strongly depends on the secondary electron emission. According to Auger neutralization, the secondary electron emission from the surface state also depends on the energy band structure and the surface state density. Thus, we have come to a conclusion that the reduction in the firing voltage by doping the Li on the MgO layer has a strong correlation with the reduction in work function or energy band structure, as shown in Fig. 6.

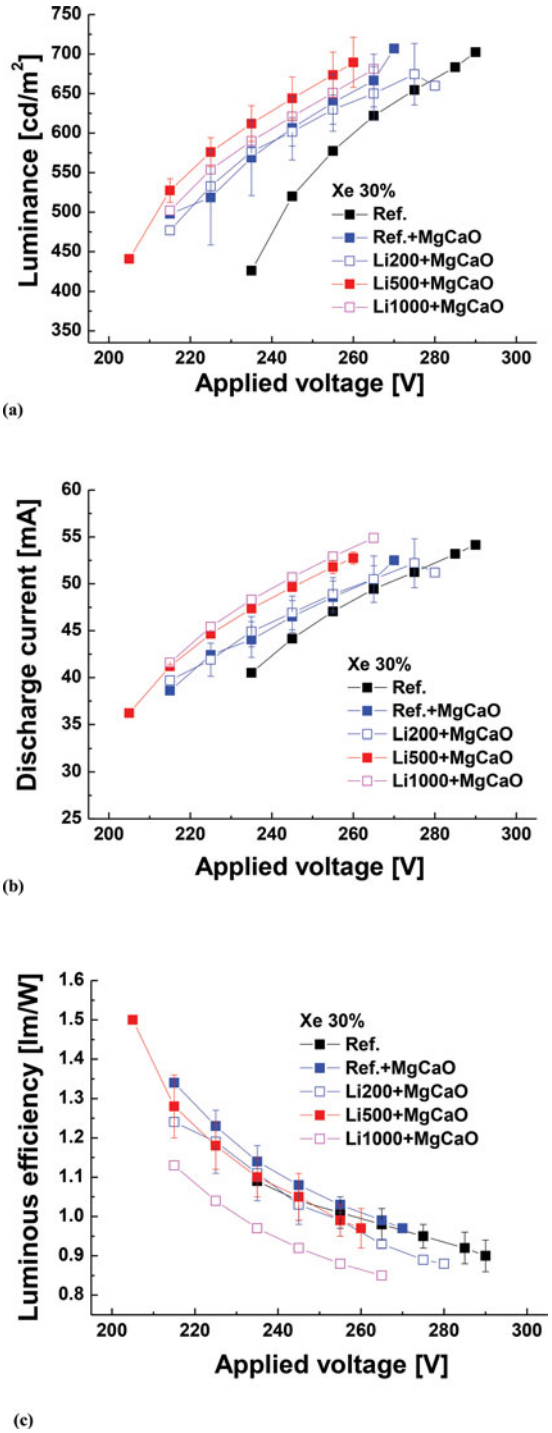

Figure 5. Changes in (a) luminance, (b) discharge current, and (c) luminous efficiency measured test panel with high Xe (= 30%) under various MgO surface conditions, that is, undoped MgO surface without MgCaO crystal powders (Ref.), undoped MgO surface with MgCaO crystal powders (Ref. + MgCaO), Li-doped (200 ppm) MgO surface with MgCaO crystal powders (Li200 + MgCaO), Li-doped (500 ppm) MgO surface with MgCaO crystal powders (Li500 + MgCaO), and Li-doped (1000 ppm) MgO surface with MgCaO crystal powders (Li1000+MgCaO).

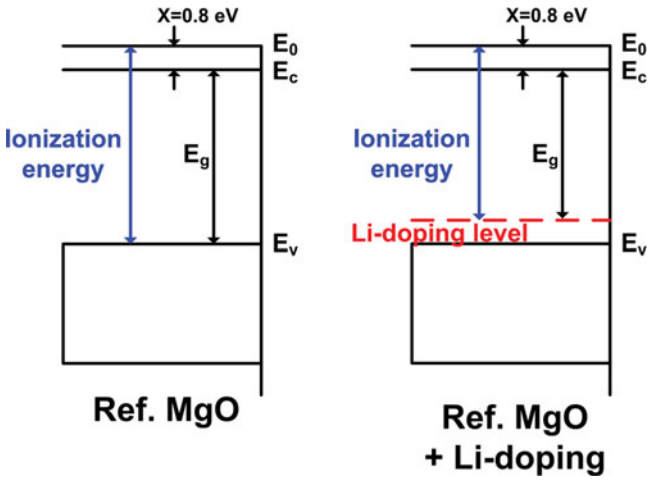

Figure 6. Schematic model of energy band for two different MgO this films, *i.e.*, Li-doped and undoped MgO thin films.

Accordingly, our experiment confirms that the modification of the conventional MgO surface by means of doping the Li and depositing the crystal functional layer such as the MgCaO crystal powders would contribute to enhancing the luminous efficiency and discharge characteristics especially under the high Xe (= 30%) gas condition in the current PDP-TVs.

4. Conclusions

This paper compares and examines the influences of the functional layer such as the MgCaO crystal powders including the doping effect such as Li on the discharge and luminous efficiency especially under the high Xe(= 30%) gas condition. The sizes of the MgCaO crystal powders are ranging from a few tens of nanometers to a few micrometers, whereas the Li doping rate in the MgO layer is changed from 200 to 1000 ppm. The corresponding firing voltage, luminance, discharge current, and luminous efficiency are measured and compared depending on various MgO layers under the high Xe(= 30%) gas condition. As a result, the maximum luminous efficacy of about 40% improvement is obtained when adopting the Li-500 ppm doped MgO layer coated by MgCaO crystal powders under high Xe (= 30%) gas condition.

Funding

This work was supported by the National Research Foundation of Korea (NRF) grant funded by the Korea government (MOE) (No. 2016R1D1A1B03933162).

References

[1] Okada, T., Naoi, T., & Yoshioka, T. (2009). *J. Appl. Phys.*, *105*, 113304.
[2] Jung, E. Y, Park, C. S, & Sohn, S. H. (2012). *Mol. Cryst. Liq. Cryst.*, *564*, 43.
[3] Jung, E. Y, Park, C. S, Hong, T. E, & Sohn, S. H. (2014). *Jap. J. Appl. Phys.*, *53*, 036002.
[4] Motoyama, Y., Murakami, Y., Seki, M., Kurauchi, T., & Kikuchi, N. (2007). *IEEE Trans. Electron Devices*, *54*, 1308.
[5] Okada, T. & Yoshioka, T. (2008). *Appl. Phys. Lett.*, *93*, 171501.

[6] Hong, M., Kortan, A. R, Chang, P., Huang, Y. L, Chen, C. P, Chou, H. Y, Lee, H. Y, Kwo, J., M. W. Chu, Chen, C. H, Goncharova, L. V, Garfunkel, E., & Gustafsson, T. (2005). *Appl. Phys. Lett.*, *87*, 251902.
[7] Naoi, T., Lin, H., Hirota, A., Otani, E., & Amemiya, K. (2009). *J. Soc. Inf. Disp.*, *17*, 113.
[8] Hashimoto, K., Itakura, S., Sakata, K., Tokunaga, T., Ishizuka, M., Iwaoka, S., & Saegusa, N. (2009). *J. Soc. Inf. Disp.*, *17*, 107.
[9] Park, C. S. & Tae, H. S. (2010). *Mol. Cryst. Liq. Cryst.*, *531*, 73.
[10] Park, C. S, Tae, H. S, Jung, E. Y, Seo, J. H, & Shin, B. J. (2010). *IEEE Trans. Plasma Science*, *38*, 2439.
[11] Kim, J. H, Park, C. S, Park, H. D, Tae, H. S, & Lee, S. H. (2013). *J. Nanoscience & Nanotechnology*, *13*, 3270.
[12] Oversluizen, G., S. T. de Zwart, & Dekker, T. (2008). *J. Appl. Phys.*, *103*, 13301.
[13] Bae, H. S, Kim, J. K, Jung, H. Y, Lim, J. K, & Whang, K. W. (2007). *J. Appl. Phys.*, *102*, 123308.
[14] Park, C. S, Tae, H. S, Kwon, Y. K, & Heo, E. G. (2008). *IEEE Trans. Plasma Science*, *36*, 1925.
[15] Park, K. H, Tae, H. S, Jeong, H. S, Hur, M., & Heo, E. G. (2009). *J. Soc. Inf. Disp.*, *17*, 61.
[16] Park, H. D, Kim, J. H, Shin, B. J, Seo, J. H, Tae, H. S. (2015). *AIP Advances*, *5*, 057119.
[17] Park, C. S & Tae, H. S. (2009). *IEICE Trans. Electron.*, *E92-C*, 898.
[18] Jang, S. K & Tae, H. S. (2009). *IEEE Trans. Plasma Science*, *37*, 334.